한국소음진동공학회 2011년 춘계학술대회논문집, pp.816~820

Increase of Side-lobe Level Difference of Spherical Microphone Array by Implementing MEMS Sensor

이재형* · 최시홍** · 최종수†

Jaehyung Lee*, Sihong Choi and Jong-Soo Choi†**

Key Words : Spherical Array, MEMS Microphone, Side-Lobe Level, Spherical Harmonic Decomposition, Beamforming

ABSTRACT

A method for increasing the difference of side-lobe level in spherical microphone array is presented. In array signal processing, it is known that narrow interval between sensors can increase the difference between main lobe and side-lobe of array response which eventually increase the source recognition capability. Recent commercial array being used, however, have shown certain limitation in using the number of sensors due to its costs and geometrical size of array. To overcome this problem, we have adapted MEMS sensors into spherical microphone array. To check out the improvement, two different types of spherical microphone array were designed. One array is composed with 32 regular instrument microphones and the other one is 85 MEMS sensors. Simulation and experiments were conducted on a sinusoidal noise source with two arrays. The time history data were analyzed with spherical harmonic decomposition and beamforming technique. 85 MEMS sensors array showed the improved side-lobe level suppression by more than 4 dB above the frequency content of 2 kHz compared to 32-sensor array.

초 록

본 논문은 구형 마이크로폰 어레이의 부엽 레벨의 차를 증가시키기 위한 방법에 대한 연구 내용을 다루었다. 일반적인 어레이 신호처리에서 마이크로폰을 조밀하게 배치함으로써 어레이 응답에서의 주엽과 부엽 간의 차이를 늘릴 수 있고 어레이의 소음원 판별 능력을 증가시킨다. 최근 사용되고 있는 상용 에레이들은 제작 단가와 어레이의 크기 때문에 센서의 수를 늘리는데 한계를 보이고 있다. 이런 문제를 극복하기 위해 본 연구에서는 MEMS 센서를 이용하여 구형 어레이에 적용하였다. 구형 마이크로폰 어레이를 이용한 시뮬레이션과 실험을 통해 정현파 소음원을 측정하였다. 실험을 위해 32 개의 일반 측정용 마이크로폰을 이용한 어레이와 85 개의 MEMS 마이크로폰을 이용한 구형 어레이를 제작하였다. 구형 조화 분해기법과 빔형성기법을 이용하여 측정 데이터를 분석하였다. 2 kHz 이상의 소음원에 대하여 MEMS 마이크로폰 어레이가 4 dB 이상의 부엽 저감 능력을 가지는 것을 확인하였다.

1. Introduction

In this paper, a spherical microphone array has been developed to increase its sound source recognition capability by implementing large number of MEMS sensors. An array capability can be represented with both beamwidth and side-lobe suppression level appeared in array response. Beamwidth at -3 dB of main lobe shows the resolution of the array and the difference of level between main lobe and side lobe indicates how well the array distinguish real noise source from ghost source.

†Chungnam National University, Dept. of Aerospace Eng.
E-mail : jchoi@cnu.ac.kr
Tel : +82-42-821-6683, Fax : +82-42-825-9225
* Chungnam National University, Dept. of Aerospace Eng.
** Korean Air

Commercial spherical array has shown an effort of sizing an array to fit measurement conditions such as indoor or vehicle interior noise.[1] Considering such sound field, the array should be small enough not to block wave propagation and large enough to house sensors inside. Such spherical array has usually used instrument microphone which provides flat sensitivity over broad frequency band up to 20 kHz. Though its good performance, the instrument microphone has a volume itself including amplifier, wire and so on. Consequently, the number of sensor should be limited when being used in spherical array.

The primary objective of the present work is to estimate the side-lobe level difference due to the distribution of sensors. Next, design and construction of spherical array by implementing MEMS sensors is described. Description of experiment is followed by comparison of simulation and experimental results.

2. Theoretical Background

2.1 Spherical Harmonic Decomposition

The incoming sound is assumed to be the infinite series of plane waves. Then, sound wave received from all direction can be Fourier transformed on the sphere.[2, 3] The spherical Fourier transform of f is expressed as

$$\tilde{f}_{nm} = \int_0^{2\pi} \int_0^{\pi} f(\theta,\phi) Y_n^{m*}(\theta,\phi) d\theta d\phi \qquad (1)$$

where spherical harmonics of order n and degree m are defined by

$$Y_n^m(\theta,\phi) = \sqrt{\frac{(2n+1)}{4\pi}\frac{(n-m)!}{(n+m)!}} P_n^m(\cos\theta) e^{im\phi}. \qquad (2)$$

The associated Legendre function P_n^m represents standing spherical wave in θ and $e^{im\phi}$ traveling spherical wave in ϕ.

2.2 Sound Pressure on Sphere

The incident plane wave arriving from a direction (θ_l, ϕ_l) with amplitude w on the sphere is given by

$$p_l(kr,\theta,\phi) = \sum_{n=0}^{\infty} \sum_{m=-n}^{n} w(\theta_l,\phi_l) \tilde{b}_n(kr,ka) Y_n^{m*}(\theta_l,\phi_l) Y_n^m(\theta,\phi) \qquad (3)$$

where k is the wave number, r is the radius of the sphere. The subscript l means the direction of arrival of sound wave. The coefficient $\tilde{b}_n$ is

$$\tilde{b}_n(kr,ka) = \begin{cases} 4\pi(-i)^n \left(j_n(kr) - \frac{j'_n(kr)}{h'_n(kr)} h_n(kr) \right) & \text{rigid surface.} \\ 4\pi(-i)^n j_n(kr) & \text{open surface} \end{cases} \qquad (4)$$

The coefficient of Fourier transform of pressure is found by

$$\tilde{p}_{l_{nm}} = w(\theta_l,\phi_l) \tilde{b}_n(kr,ka) Y_n^{m*}(\theta_l,\phi_l). \qquad (5)$$

2.3 Beamforming

The sound field is analyzed by using beamforming method. Beamforming provides a spatial filter response at a certain point by adding array signal associated with the propagation direction. The power distribution is calculated from the product of array steering vector and Fourier transformed pressure.[5, 6]

3. Experiment

Two spherical microphone arrays were built and experiments were conducted. One spherical array with a radius of 0.12 m has 32 instrument microphones. The configuration of array is like the vertex of a soccer ball which has euqi-distance between each other. The other array with 85 sensors uses MEMS microphones and has linear distribution along altitude(Fig. 1). Sensors are evenly distributed along each altitude, on the other hand, angular distance between each altitude is not even. The coordinate of the both array are referred to the appendix.

When sound field was measured with 32-sensor array, four National Instrument (NI) PXI-4472 data acquisition boards were used. In case of 85-sensor array, other data acquisition system was designed with 8 multiplexers (MUX). Each MUX handles a set of 8 channels and is controlled by a NI USB-6259 DAQ board. Each set of acoustic signal was sampled sequentially while one reference microphone located on pole of the sphere collecting the data as every moment each set of channel was acquired.

Several frequencies of sinusoidal noises were measured in an anechoic chamber and the array signal was processed by using spherical harmonic decomposition. Noise was measured 1 m away from the spherical array. Furthermore, since the speaker is practically a point source, measurement was made to observe the effect due to the distance change.

4. Discussion

Experimental and simulation results of 32-sensor array and 85-sensor array are compared. Maximum Side-lobe Level (MSL) from the frequency of 500 Hz up to 8000 Hz is shown in Fig. 2. MSL result indicates the difference between main-lobe level and next largest side-lobe level which means that the larger the MSL, the better the array distinguish real noise sources from imaginary ones. At 500 Hz and 1000 Hz, 32-sensor array and 85-sensor array does not show much difference in MSL. From 2000 Hz up to 8000 Hz, MSL shows more than 4 dB difference. Though 85-sensor array shows large difference over all frequency bands, any typical trend is not observed.

In Fig. 3, beamwidth from both arrays shows similar results. It is because the beamwidth is mainly dependent on the size of the array rather than the number of sensors or spacing between sensors. However, if the size of the array increases assuming of using the same number of sensors, the spacing becomes wider which, at the same time, gives a negative effect of degrease in MSL as shown in Fig. 4.

MSL of 85-sensor array measurement along the distance changes is shown in Fig. 5. The simulation result means that the incident sound wave is coming from a far field. Measurement above 2000 Hz shows similar level change compared to the simulation. Experimental results at 2000 Hz and 4000 Hz show 2 dB less than simulation.

Fig. 1. Spherical Array with 85 MEMS Sensors

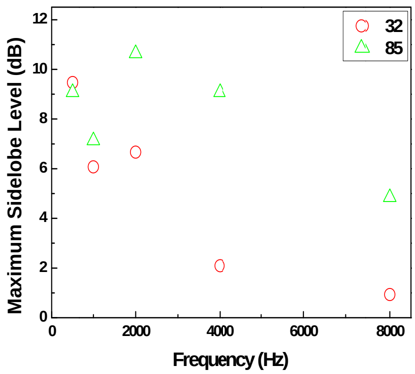

Fig. 2. MSL Results from Experiments of 32-sensor array and 85-sensor array

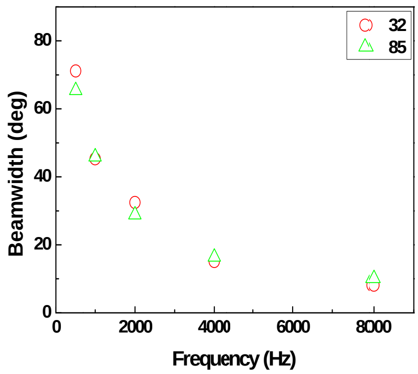

Fig. 3. Beamwidth Results from Experiments of 32-sensor array and 85-sensor array

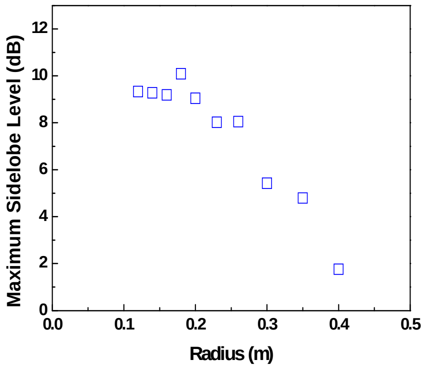

Fig. 4. Beamwidth Results from Simulation of 32-sensor with Various Radii

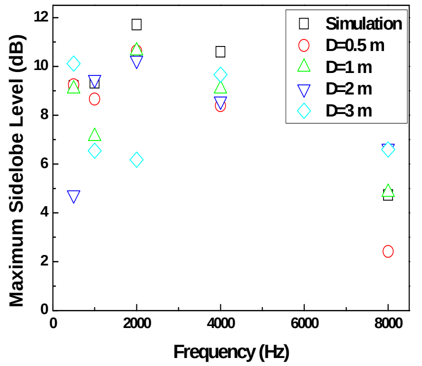

Fig. 5. MSL Results of 85-sensor array between Simulation and Experiments along with Measurement Distance Changes

4. Conclusion

This paper presented an improvement of side-lobe level suppression capability of a spherical array by using MEMS microphones. Two different type of spherical array was designed and tested with single noise source. The comparison of simulation and experimental results over various frequency contents has been made. 85-sensor array achieved good improvement in side-lobe level difference while beamwidth was observed to have no significant improvement due to the array size. MEMS microphone proved to be very practical in building a spherical array.

Acknowledgement

This work was supported by the National Research Foundation of Korea(NRF) grant funded by the Korea government(MEST) (No. 2010-0014978). The authors thank Mr. Wook Rhee for his contribution of designing electrical components.

References

(1) Juhl, P. M., Petersen, S. O. and Hald, J., 2005, Localizing Sound Sources in 3-D Space Using Spherical Harmonic Beamforming, Proceedings of inter-noise 2005 Rio.

(2) Li, Z. and Duraiswami R., 2007, Flexible and Optimal Design of Spherical Microphone Arrays for Beamforming, IEEE Transactions on Audio, Speech and Language Processing, Vol. 15, No. 2, 2007.

(3) Choi, S., Lee, J., Choi, J.-S. and Kim, Y.-K., 2010, Optimization of Sensor Position of a Rigid Surface Spherical Beamformer, Proceedings of the KSNVE Annual Fall Conference, pp.128~129.

(4) Johnson, Don H. and Dudgeon, Dan E., 1993, Array Signal Processing: Concepts and Techniques, PTR Prentice Hall.

(5) Lee, J., Choi, J.-S., and Park, K.-C., 2004, Experiments for the Acoustic Source Localization in 2D Cavity Flow, Transactions of the Korean Society for Noise and Vibration Engineering. Vol. 14, No. 12, pp. 1241~1248.

APPENDIX

A. Coordinate of array with 23 microphones

CH	THETA	PHI	CH	THETA	PHI
1	81.4	90.0	17	123.9	89.4
2	53.4	88.7	18	166.7	115.4
3	65.9	128.6	19	99.1	119.1
4	26.3	141.5	20	133.5	145.9
5	59.5	170.0	21	94.3	160.6
6	79.7	200.8	22	119.8	190.9
7	45.4	215.0	23	152.7	219.1
8	77.8	235.0	24	114.8	231.3
9	56.4	270.5	25	133.1	269.1
10	14.6	272.8	26	95.6	269.9
11	77.1	303.8	27	114.6	309.2
12	46.7	325.4	28	153.6	327.2
13	84.4	340.1	29	120.2	349.0
14	61.4	11.3	30	96.1	20.4
15	28.6	37.8	31	133.8	34.6
16	68.9	50.5	32	99.9	57.6

B. Coordinate of array with 85 microphones

CH	THETA	PHI	CH	THETA	PHI
1	21	15	44	90	202.5
2	21	75	45	90	225
3	21	135	46	90	247.5
4	21	195	47	90	270
5	21	255	48	90	292.5
6	21	315	49	90	315
7	44	0	50	90	337.5
8	44	30	51	113	11.25
9	44	60	52	113	33.75
10	44	90	53	113	56.25
11	44	120	54	113	78.75
12	44	150	55	113	101.25
13	44	180	56	113	123.75
14	44	210	57	113	146.25
15	44	240	58	113	168.75
16	44	270	59	113	191.25
17	44	300	60	113	213.75
18	44	330	61	113	236.25
19	67	0	62	113	258.75
20	67	22.5	63	113	281.25
21	67	45	64	113	303.75
22	67	67.5	65	113	326.25
23	67	90	66	113	348.75
24	67	112.5	67	136	0
25	67	135	68	136	30
26	67	157.5	69	136	60
27	67	180	70	136	90
28	67	202.5	71	136	120
29	67	225	72	136	150
30	67	247.5	73	136	180
31	67	270	74	136	210
32	67	292.5	75	136	240
33	67	315	76	136	270
34	67	337.5	77	136	300
35	90	0	78	136	330
36	90	22.5	79	159	15
37	90	45	80	159	75
38	90	67.5	81	159	135
39	90	90	82	159	195
40	90	112.5	83	159	255
41	90	135	84	159	315
42	90	157.5	85	180	0
43	90	180			